Eur. Phys. J. C 37, 79–90 (2004)
Digital Object Identifier (DOI) 10.1140/epjc/s2004-01987-9

THE EUROPEAN PHYSICAL JOURNAL C

Measurement of the np total cross section difference $\Delta\sigma_{\rm L}(np)$ at 1.39, 1.69, 1.89 and 1.99 GeV

V.I. Sharov[1,a], N.G. Anischenko[1], V.G. Antonenko[2], S.A. Averichev[1], L.S. Azhgirey[3], V.D. Bartenev[1], N.A. Bazhanov[3], A.A. Belyaev[5], N.A. Blinov[1], N.S. Borisov[3], S.B. Borzakov[6], Yu.T. Borzunov[1], Yu.P. Bushuev[1], L.P. Chernenko[6], E.V. Chernykh[1], V.F. Chumakov[1], S.A. Dolgii[1], A.N. Fedorov[3], V.V. Fimushkin[1], M. Finger[3,7], M. Finger, Jr.[3], L.B. Golovanov[1], G.M. Gurevich[8], A. Janata[3], A.D. Kirillov[1], V.G. Kolomiets[3], E.V. Komogorov[1], A.D. Kovalenko[1], A.I. Kovalev[4], V.A. Krasnov[1], P. Krstonoshich[3], E.S. Kuzmin[3], V.P. Ladygin[1], A.B. Lazarev[3], F. Lehar[9], A. de Lesquen[9], M.Yu. Liburg[1], A.N. Livanov[1], A.A. Lukhanin[5], P.K. Maniakov[1], V.N. Matafonov[3], E.A. Matyushevsky[1], V.D. Moroz[1], A.A. Morozov[1], A.B. Neganov[3], G.P. Nikolaevsky[1], A.A. Nomofilov[1], Tz. Panteleev[6,10], Yu.K. Pilipenko[1], I.L. Pisarev[3], Yu.A. Plis[3], Yu.P. Polunin[2], A.N. Prokofiev[4], V.Yu. Prytkov[1], P.A. Rukoyatkin[1], V.A. Schedrov[4], O.N. Schevelev[3], S.N. Shilov[3], R.A. Shindin[1], M. Slunečka[3,7], V. Slunečková[3], A.Yu. Starikov[1], G.D. Stoletov[3,†], L.N. Strunov[1], A.L. Svetov[1], Yu.A. Usov[3], T. Vasiliev[1], V.I. Volkov[1], E.I. Vorobiev[1], I.P. Yudin[11], I.V. Zaitsev[1], A.A. Zhdanov[4], V.N. Zhmyrov[3]

[1] Joint Institute for Nuclear Research, Veksler and Baldin Laboratory of High Energies, 141980 Dubna, Russia
[2] Russian Scientific Center "Kurchatov Institute", 123182 Moscow, Russia
[3] Joint Institute for Nuclear Research, Dzhelepov Laboratory of Nuclear Problems, 141980 Dubna, Russia
[4] Peterburg Nuclear Physics Institute, High Energy Physics Division, 188350 Gatchina, Russia
[5] Kharkov Institute of Physics and Technology, 310108 Kharkov, Ukraine
[6] Joint Institute for Nuclear Research, Frank Laboratory of Neutron Physics, 141980 Dubna, Russia
[7] Charles University, Faculty of Mathematics and Physics, V Holešovičkách 2, 180 00 Praha 8, Czech Republic
[8] Institute for Nuclear Research, Russian Academy of Sciences, 117312 Moscow, Russia
[9] DAPNIA, CEA/Saclay, 91191 Gif-sur-Yvette Cedex, France
[10] Institute for Nuclear Research and Nuclear Energy, Bulgarian Academy of Sciences, Tsarigradsko shaussee boulevard 72, 1784 Sofia, Bulgaria
[11] Joint Institute for Nuclear Research, Laboratory of Particle Physics, 141980 Dubna, Russia

Received: 13 May 2004 /
Published online: 12 August 2004 – © Springer-Verlag / Società Italiana di Fisica 2004

Abstract. New accurate results of the neutron-proton spin-dependent total cross section difference $\Delta\sigma_{\rm L}(np)$ at the neutron beam kinetic energies 1.39, 1.69, 1.89 and 1.99 GeV are presented. Measurements were carried out in 2001 at the Synchrophasotron of the Veksler and Baldin Laboratory of High Energies of the Joint Institute for Nuclear Research. A quasi-monochromatic neutron beam was produced by break-up of extracted polarized deuterons. The deuteron (and hence neutron) polarization direction was flipped every accelerator burst. The vertical neutron polarization direction was rotated onto the neutron beam direction and longitudinally (L) polarized neutrons were transmitted through a large proton L-polarized target. The target polarization vector was inverted after 1–2 days of measurements. The data were recorded for four different combinations of the beam and target parallel and antiparallel polarization directions at each energy. A fast decrease of $\Delta\sigma_{\rm L}(np)$ with increasing energy above 1.1 GeV was confirmed. The structure in the $\Delta\sigma_{\rm L}(np)$ energy dependence around 1.8 GeV, first observed from our previous data, seems to be well pronounced. The new results are also compared with model predictions and with phase shift analysis fits. The $\Delta\sigma_{\rm L}$ quantities for isosinglet state I = 0, deduced from the measured $\Delta\sigma_{\rm L}(np)$ values and the known $\Delta\sigma_{\rm L}(pp)$ data, are also given. The results were completed by the measurements of unpolarized total cross sections $\sigma_{0\rm tot}(np)$ at 1.3, 1.4 and 1.5 GeV and $\sigma_{0\rm tot}(n{\rm C})$ at 1.4 and 1.5 GeV. These data were obtained using the same apparatus and high intensity unpolarized deuteron beams were extracted either from the Synchrophasotron, or from the Nuclotron.

[a] e-mail: sharov@sunhe.jinr.ru
[†] Deceased

1 Introduction

In this paper are presented the new results of the spin-dependent neutron-proton total cross section difference $\Delta\sigma_{\rm L}(np)$, measured in 2001 with a quasi-monochromatic polarized neutron beam and a polarized proton target (PPT). The $\Delta\sigma_{\rm L}(np)$ values were obtained at the central neutron beam kinetic energies of 1.39, 1.69, 1.89 and 1.99 GeV. In addition, spin-averaged total cross sections $\sigma_{0\rm tot}(np)$ at 1.3, 1.4 and 1.5 GeV and $\sigma_{0\rm tot}(nC)$ at 1.4 and 1.5 GeV were measured using an unpolarized neutron beam and unpolarized targets.

The measurements were carried out within the JINR project "DELTA-SIGMA experiment". The aim of this experimental program is to obtain data sets of np observables over the Dubna neutron energy region, sufficient to perform a direct reconstruction of the scattering amplitudes (DRSA) in the forward direction. To determine the imaginary and real parts of the np and the isosinglet (I = 0) amplitudes at $\theta = 0$ requires a knowledge of six independent np quantities (at least), assuming that the isotriplet (I = 1) system is known. For several measurements the polarized neutron beam and PPT are needed.

The measurements of the total cross section differences over the Dubna Synchrophasotron neutron beam energy range have been proposed in the early 1990 [1,2]. The successful data taking runs were carried out in 1995 and 1997 and the $\Delta\sigma_{\rm L}(np)$ values were measured at 1.19, 1.59, 1.79, 2.20, 2.49, and 3.66 GeV [3–6].

The free polarized neutron beam was produced by break-up of polarized deuterons accelerated by the Synchrophasotron of the Veksler and Baldin Laboratory of High Energies (VBLHE) at the Joint Institute for Nuclear Research (JINR) in Dubna. This accelerator provides the highest energy (3.7 GeV) polarized neutron beam, that can be reached at the present moment. New polarized neutron beam line with the desirable parameters was constructed and tested [7,8]. The unpolarized deuteron beams were extracted either from the Synchrophasotron, or from the Nuclotron of VBLHE and provided free unpolarized neutrons in the same beam line.

For the purposes of $\Delta\sigma_{\rm L}(np)$ measurements, a large Argonne-Saclay PPT was reconstructed at Dubna [9–11]. In 1997, a new PPT polarizing solenoid [12] was developed in VBLHE.

A set of dedicated neutron detectors with corresponding electronics were utilized. The CAMAC data acquisition system and the on-line program were developed. A powerful neutron shielding and a neutron spin rotator were implemented. The apparatus was continuously improved and completed.

The spin-dependent nucleon-nucleon (NN) observables $\Delta\sigma_{\rm L}$ and $\Delta\sigma_{\rm T}$ are defined as the difference of the total cross sections for antiparallel and parallel beam and target polarizations, oriented either longitudinally (L), or transversally (T) with respect to the beam direction.

The NN total cross section differences $\Delta\sigma_{\rm L}$ and $\Delta\sigma_{\rm T}$, together with the spin-average total cross section $\sigma_{0\rm tot}$ are measured in pure inclusive transmission experiments. They are linearly related with three non-vanishing imaginary parts of the NN forward scattering amplitudes via optical theorems and allow to reconstruct directly these imaginary parts. The data are also used to check the predictions of available dynamic models and provide an important contribution to databases of phase-shift analyses (PSA). From the measured $\Delta\sigma_{\rm L,T}(np)$ values it is possible to deduce the $\Delta\sigma_{\rm L,T}$ nucleon-nucleon isosinglet (I = 0) part, using the existing pp (isotriplet I = 1) results.

The total cross section differences $\Delta\sigma_{\rm L,T}$ for pp scattering were first measured at the ANL-ZGS and then at TRIUMF, in PSI, at LAMPF, Saturne II and in Fermilab. Results were obtained in the energy range from 0.2 to 12 GeV and at 200 GeV. Measurements with incident charged particles need an experimental set-up different from neutron-proton experiments, due to the contribution of electromagnetic interactions. Existing $\Delta\sigma_{\rm L,T}(pp)$ results were discussed in the review [13] and in references therein.

$\Delta\sigma_{\rm L}(pn)$ results from 0.51 to 5.1 GeV were deduced for the first time in 1981 from the $\Delta\sigma_{\rm L}(pd)$ and $\Delta\sigma_{\rm L}(pp)$ measurements at the ANL-ZGS [14]. These pn results were omitted in many existing PSA databases, due to uncertainties in the Glauber-type rescattering corrections. They were discussed in [3,4,13].

$\Delta\sigma_{\rm T}(np)$ and $\Delta\sigma_{\rm L}(np)$ results were obtained at 11 and 10 energies, respectively, in the energy range from 0.31 to 1.10 GeV, using free polarized neutrons at Saturne II [15–17]. The Saclay results were soon followed by PSI measurements [18] at 7 energy bins from 0.180 to 0.537 GeV, using a continuous neutron energy spectrum. The PSI and Saclay sets allowed to deduce imaginary parts of np and I = 0 spin-dependent forward scattering amplitudes [13, 17]. Only $\Delta\sigma_{\rm L}(np)$ has been measured at five energies between 0.484 and 0.788 GeV at LAMPF [19]. There, a quasi-monoenergetic polarized neutron beam was produced in $pd \to n+X$ scattering of longitudinally polarized protons.

At low energies, $\Delta\sigma_{\rm L}(np)$ was measured at 66 MeV at the PSI injector [20], and at 16.2 MeV in Charles University, Prague [21]. $\Delta\sigma_{\rm T}(np)$ was determined in Triangle Universities Nuclear Laboratory (TUNL, Durham NC) at 9 energies between 3.65 and 11.6 MeV [22], and at 16.2 MeV in Prague [23]. Finally, in TUNL $\Delta\sigma_{\rm L}(np)$ was measured at 6 energies between 4.98 and 19.7 MeV [24] and $\Delta\sigma_{\rm T}(np)$ at 3 other energies between 10.7 and 17.1 MeV [25].

At high energies the $\Delta\sigma_{\rm L}(np)$ results, using free polarized neutrons were obtained at the JINR Synchrophasotron only. The Dubna results smoothly connect with the existing data at lower energies. The $-\Delta\sigma_{\rm L}(np)$ energy dependence shows a fast decrease to zero above 1.1 GeV and a structure around 1.8 GeV. Values of the I = 0 part of $\Delta\sigma_{\rm L}$ are also presented. The data are compared with model predictions and with the PSA fits.

In Sect. 2 a brief determination of observables is given. Section 3 describes the method of the measurements. The essential details concerning the beam, the polarimeters, the experimental set-up and PPT are given in Sect. 4. Data acquisition and analyses are described in Sect. 5. Results and their discussion are presented in Sect. 6.

2 Determination of observables

Throughout this paper we use the NN formalism and the notations for the elastic nucleon-nucleon scattering observables from [26].

The general expression of the total cross section for a polarized nucleon beam transmitted through a PPT, with arbitrary directions of beam and target polarizations, $\mathbf{P}_{\rm B}$ and $\mathbf{P}_{\rm T}$, respectively, was first deduced in [27,28]. Taking into account fundamental conservation laws, it is written in the form:

$$\sigma_{\rm tot} = \sigma_{0\rm tot} + \sigma_{1\rm tot}(\mathbf{P}_{\rm B}, \mathbf{P}_{\rm T}) + \sigma_{2\rm tot}(\mathbf{P}_{\rm B}, \mathbf{k})(\mathbf{P}_{\rm T}, \mathbf{k}), \quad (2.1)$$

where $\mathbf{k}$ is a unit vector in the direction of the beam momentum. The term $\sigma_{0\rm tot}$ is the total cross section for unpolarized particles, $\sigma_{1\rm tot}$, $\sigma_{2\rm tot}$ are the spin-dependent contributions. They are related to the measurable observables $\Delta\sigma_{\rm T}$ and $\Delta\sigma_{\rm L}$ by:

$$-\Delta\sigma_{\rm T} = 2\sigma_{1\rm tot}, \quad (2.2)$$
$$-\Delta\sigma_{\rm L} = 2(\sigma_{1\rm tot} + \sigma_{2\rm tot}), \quad (2.3)$$

called "total cross section differences". The negative signs for $\Delta\sigma_{\rm T}$ and $\Delta\sigma_{\rm L}$ in (2.2) and (2.3) correspond to the usual, although unjustified, convention in the literature. The total cross section differences are measured with either parallel or antiparallel beam and target polarization directions. Polarization vectors are transversally oriented with respect to $\mathbf{k}$ for $\Delta\sigma_{\rm T}$ measurements and longitudinally oriented for $\Delta\sigma_{\rm L}$ experiments. Only $\Delta\sigma_{\rm L}$ measurements are treated below, but the formulae for $\Delta\sigma_{\rm T}$ (2.2) are similar.

For $\mathbf{P}_{\rm B}^{\pm}$ and $\mathbf{P}_{\rm T}^{\pm}$, all oriented along $\mathbf{k}$, we obtain four total cross sections:

$$\sigma(\rightrightarrows) = \sigma(++) = \sigma_{0\rm tot} + |P_{\rm B}^{+} P_{\rm T}^{+}|\ (\sigma_{1\rm tot} + \sigma_{2\rm tot}), \quad (2.4a)$$
$$\sigma(\leftrightarrows) = \sigma(-+) = \sigma_{0\rm tot} - |P_{\rm B}^{-} P_{\rm T}^{+}|\ (\sigma_{1\rm tot} + \sigma_{2\rm tot}), \quad (2.4b)$$
$$\sigma(\rightleftarrows) = \sigma(+-) = \sigma_{0\rm tot} - |P_{\rm B}^{+} P_{\rm T}^{-}|\ (\sigma_{1\rm tot} + \sigma_{2\rm tot}), \quad (2.4c)$$
$$\sigma(\leftleftarrows) = \sigma(--) = \sigma_{0\rm tot} + |P_{\rm B}^{-} P_{\rm T}^{-}|\ (\sigma_{1\rm tot} + \sigma_{2\rm tot}). \quad (2.4d)$$

The signs in brackets correspond to the $\mathbf{P}_{\rm B}$ and $\mathbf{P}_{\rm T}$ directions with respect to $\mathbf{k}$, in this order. In principle, an arbitrary pair of one parallel and one antiparallel beam and target polarization directions determines $\Delta\sigma_{\rm L}$. By using two independent pairs, we remove an instrumental asymmetry term (IA).

In the following, we will consider the neutron beam and the proton target. Since the $\mathbf{P}_{\rm B}$ direction could be reversed at every cycle of the accelerator, it is preferable to calculate $\Delta\sigma_{\rm L}$ from the pairs $(\rightrightarrows)$, $(\leftrightarrows)$, and $(\rightleftarrows)$, $(\leftleftarrows)$, measured with the same $\mathbf{P}_{\rm T}$ orientation. This eliminates long-time efficiency fluctuations of the neutron detectors. The spin-averaged term $\sigma_{0\rm tot}$ drops out when taking the difference, and one obtains:

$$-\Delta\sigma_{\rm L}(P_{\rm T}^{+}) = 2\ (\sigma_{1\rm tot} + \sigma_{2\rm tot})^{+} = \frac{2\ [\sigma(\rightrightarrows) - \sigma(\leftrightarrows)]}{(|P_{\rm B}^{+}| + |P_{\rm B}^{-}|)\ |P_{\rm T}^{+}|}, \quad (2.5a)$$

$$-\Delta\sigma_{\rm L}(P_{\rm T}^{-}) = 2\ (\sigma_{1\rm tot} + \sigma_{2\rm tot})^{-} = \frac{2\ [\sigma(\leftleftarrows) - \sigma(\rightleftarrows)]}{(|P_{\rm B}^{+}| + |P_{\rm B}^{-}|)\ |P_{\rm T}^{-}|}, \quad (2.5b)$$

Measured $-\Delta\sigma_{\rm L}$, i.e. the effect of the difference between total cross sections for parallel and antiparallel orientations of beam and target polarizations, are proportional to the mean value of the beam polarizations $|P_{\rm B}^{+}|$ and $|P_{\rm B}^{-}|$:

$$|P_{\rm B}| = \frac{1}{2}(|P_{\rm B}^{+}| + |P_{\rm B}^{-}|). \quad (2.6)$$

The $|P_{\rm B}|$ value is well known as a function of time, since it is continuously monitored by a beam polarimeter.

Each of relations (2.5a) and (2.5b) contains a hidden contribution from the instrumental asymmetry IA, caused mainly by a misalignment of the neutron detector counters (see below). The value of IA is given as:

$$\mathrm{IA} = \frac{1}{2}[\Delta\sigma_{\rm L}(P_{\rm T}^{+}) - \Delta\sigma_{\rm L}(P_{\rm T}^{-})]. \quad (2.7)$$

IA cancels out, giving the final results as a simple average

$$\Delta\sigma_{\rm L} = \frac{1}{2}[\Delta\sigma_{\rm L}(P_{\rm T}^{+}) + \Delta\sigma_{\rm L}(P_{\rm T}^{-})]. \quad (2.8)$$

The scattering matrix used contains the invariant amplitudes a, b, c, d and e, as defined in [26,13]. The formalism linearly relates $\sigma_{0\rm tot}$, $\Delta\sigma_{\rm T}$ and $\Delta\sigma_{\rm L}$ to the imaginary parts of the three independent forward scattering amplitudes $a+b$, c and d [26] via optical theorems:

$$\sigma_{0\rm tot} = (2\pi/K)\ \Im m\ [a(0) + b(0)], \quad (2.9)$$
$$-\Delta\sigma_{\rm T} = (4\pi/K)\ \Im m\ [c(0) + d(0)], \quad (2.10)$$
$$-\Delta\sigma_{\rm L} = (4\pi/K)\ \Im m\ [c(0) - d(0)], \quad (2.11)$$

where K is the wave number. For the amplitudes it holds: $a(0) - b(0) = c(0) + d(0)$ and $e(0) = 0$. The optical theorems always provide the absolute amplitudes, as discussed in [29–31]. From (2.9) to (2.11) the partial DRSA analysis unambigously determines the imaginary parts of the non-vanishing amplitudes for any NN isospin.

Using the measured $\Delta\sigma(np)$ values and the existing $\Delta\sigma(pp)$ data at the same energy, one can deduce $\Delta\sigma_{\rm L,T}(\mathrm{I}=0)$ as:

$$\Delta\sigma_{\rm L,T}(\mathrm{I}=0) = 2\Delta\sigma_{\rm L,T}(np) - \Delta\sigma_{\rm L,T}(pp). \quad (2.12)$$

3 Methods of measurement

In the transmission experiment we measure the part of incident beam particles, which remains in the beam after its passage through the target. For the experiments with incident neutrons this measurement is always relative. The neutron beam has a circular profile, formed by the preceeding beam collimators. The neutron flux out of the collimator diameter is considered to be zero. The neutron beam intensity is monitored by neutron beam monitors,

placed upstream from the target. The PPT material consists of small beads inserted in a cylindrical container of the circular profile. The container covers the beam spot and its horizontal axis coincides with the beam axis. The transmission detectors, downstream from the target, are larger than the beam dimensions. We assume that any unscattered beam particle is detected with the same probability.

With an unpolarized beam and/or target we measure a simple transmission ratio. If $N_{\rm in}$ is the number of neutrons entering the target and $N_{\rm out}$ is the number of neutrons transmitted in a counter array of solid angle Ω, then the total cross section $\sigma_{\rm tot}(\Omega) = \sigma_{0\rm tot}(\Omega)$ is related to measured quantities:

$$\frac{N_{\rm out}}{N_{\rm in}} = \exp\bigl(-\sigma_{0\rm tot}(\Omega) \times n \times d\bigr) \ , \qquad (3.1)$$

where n is the number of all target atoms per cm^3, d is the target length and $N_{\rm out}/N_{\rm in}$ is the simple transmission ratio. The number of counts of the beam monitor M and of the transmission counter T depend on the efficiency η of each detector, i.e. $M = N_{\rm in} \times \eta(M)$ and $T = N_{\rm out} \times \eta(T)$. The extrapolation of $\sigma_{0\rm tot}(\Omega)$ towards $\Omega = 0$ gives the unpolarized total cross section $\sigma_{0\rm tot}$.

In the $\Delta\sigma_{\rm L}(\Omega)$ measurements with a completely filled target, only the number of polarizable hydrogen atoms $n_{\rm H}$ is important, because $\sigma_{\rm tot}(\Omega)$ depends on the polarizations $P_{\rm B}^{\pm}$ and $P_{\rm T}^{\pm}$ as shown in (2.4). If one sums up the events taken with one fixed target polarizations $P_{\rm T}^{+}$ or $P_{\rm T}^{-}$ and using (2.5a) or (2.5b), the double transmission ratios of the measurements with the averaged $P_{\rm B}$ from (2.6) for the two $\mathbf{P}_{\rm T}$ directions become

$$\frac{N_{\rm out}(++)/N_{\rm in}(++)}{N_{\rm out}(-+)/N_{\rm in}(-+)} = \exp\ (-\Delta\sigma_{\rm L}(\Omega)\ |P_{\rm B}\ P_{\rm T}^{+}|\ n_{\rm H}\ d) \qquad (3.3a)$$

$$\frac{N_{\rm out}(--)/N_{\rm in}(--)}{N_{\rm out}(+-)/N_{\rm in}(+-)} = \exp\ (-\Delta\sigma_{L}(\Omega)\ |P_{\rm B}\ P_{\rm T}^{-}|\ n_{\rm H}\ d) \ . \qquad (3.3b)$$

We use here the notation of (2.4).

Thus the neutron detector efficiencies drop out. In the following we put $N = N_{\rm out}/N_{\rm in}$ depending on $\mathbf{P}_{\rm B}$ and $\mathbf{P}_{\rm T}$ combination and (3.3) provide:

$$-\Delta\sigma_{\rm L}(\Omega, P_{\rm T}^{+}) = \frac{1}{|P_{\rm B}\, P_{\rm T}^{+}|\, n_{\rm H}\, d} \times \ln\left(\frac{N(++)}{N(-+)}\right), \qquad (3.4a)$$

$$-\Delta\sigma_{\rm L}(\Omega, P_{\rm T}^{-}) = \frac{1}{|P_{\rm B}\, P_{\rm T}^{-}|\, n_{\rm H}\, d} \times \ln\left(\frac{N(--)}{N(+-)}\right). \qquad (3.4b)$$

Systematic uncertainties of the $-\Delta\sigma_{\rm L}(\Omega, P_{\rm T}^{\pm})$ values are mainly caused by the errors in the $|P_{\rm B}|$, $|P_{\rm T}^{\pm}|$ and $n_{\rm H}$. Statistical errors of $-\Delta\sigma_{\rm L}(\Omega, P_{\rm T}^{\pm})$ are given by the formula

$$\delta_{\rm stat} = \frac{1}{|P_{\rm B}\ P_{\rm T}|\ n_{\rm H}\ d} \times \sqrt{\frac{1}{M^{+}} + \frac{1}{M^{-}} + \frac{1}{T^{+}} + \frac{1}{T^{-}}} \ , \qquad (3.5)$$

where the M^{+}, M^{-} and T^{+}, T^{-} are the statictics for monitor and transmission neutron detectors with the $P_{\rm B}^{+}$ and $P_{\rm B}^{-}$ neutron beam polarizations, respectively, for a given sign of $|P_{\rm T}|$.

If $\Omega \to 0$, we obtain $\Delta\sigma_{\rm L}(\Omega) \to \Delta\sigma_{\rm L}$. For our np transmission measurement we may neglect the extrapolation of $\Delta\sigma_{\rm L}(\Omega)$ towards $\Omega = 0$ due to the small sizes of detectors [3,4,6,5]. The Saclay-Geneva (SG) PSA [30] at 1.1 GeV shows that for the angles covered by our detectors the resulting $-\Delta\sigma_{\rm L}$ value decreases by 0.04 mb, if we consider $\Delta\sigma_{\rm L}(\Omega) = \Delta\sigma_{\rm L}$.

The ratio of $n_{\rm H}$ to other target nuclei depends on the target material. The presence of carbon in the PPT beads adds the term $\sigma_{0\rm tot}({\rm C})$ in (2.4). This term is spin-independent and its contribution drops out in differences (2.5). The same occurs for ^{16}O and ^{4}He in the target and for the cryogenic envelopes.

However, there are small effects from ^{13}C and ^{3}He in the PPT which may be slightly polarized. The global contribution was estimated to be ± 0.3 % in [3,4].

4 Experimental set-up

The $\Delta\sigma_{\rm L}(np)$ experimental set-up was described in detail in our previous publications [3–6]. We mention here briefly the essential items, which are important for the data analysis and results. We also refer to the modifications and improvements of the apparatus and of experimental conditions.

Figure 1 shows both polarized deuteron and polarized free neutron beam lines [8], the two polarimeters [32,33], the beryllium target (BT) for neutron production, the collimators C1–C4, the spin rotation magnet (SRM), PPT [10–12], the neutron beam intensity monitors M1, M2, the transmission detectors T1, T2, T3 and the neutron beam profile monitor NP. The associated electronics was described in [3,4]. The system of data acquisition is based on CAMAC parallel branch highway controlled by IBM PC, using the branch driver [34]. The on-line program in "Pascal" works under DOS.

Accelerated deuterons were extracted at the beam momenta $p_{\rm d}$ of 4.29, 4.93, 5.36 and 5.57 GeV/c, known with a relative accuracy of $\approx \pm 1$ %. The average intensity of the primary polarized deuteron beam was $\approx\ 2 \times\ 10^{9}$d/cycle. It was continuously monitored, using two calibrated ionization chambers placed at the two focal points upstream of the neutron production target BT.

The beam of free quasi-monochromatic neutrons, polarized along the vertical direction, was obtained by breakup at 0° of vector polarized deuterons in BT. Neglecting the BT thickness, neutrons have a laboratory momentum $p_{\rm n} = p_{\rm d}/2$ with a momentum spread of FWHM $\simeq 5$ % [35]. This corresponds to the neutron beam energies $T_{\rm kin}(n)$ of 1.40, 1.70. 1.90 and 2.00 GeV, respectively.

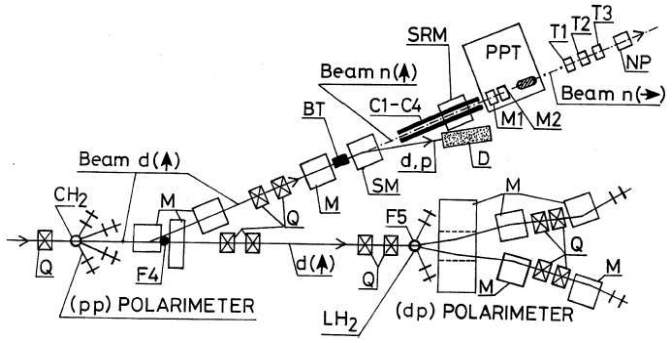

Fig. 1. Layout of the beam lines in the experimental hall (not in the scale). The meaning of the symbols: full lines ... vector polarized deuteron beams with $\mathbf{P}_{\rm B}(d)$ oriented along the vertical direction $d(\uparrow)$, dash-dotted line ... polarized neutron beam, $n(\uparrow)$ ... neutrons polarized vertically, $n(\rightarrow)$ ... neutrons polarized longitudinally, BT ... neutron production target, D ... beam-dump for charged particles, SM ... sweeping magnet, SRM ... spin rotating magnet M ... dipole magnets, Q ... quadrupoles, C1 to C4 ... neutron beam collimators, M1, M2, T1, T2, T3, neutron detectors, PPT ... polarized proton target, NP ... neutron beam profile monitor, LH_2 ... liquid hydrogen target of the dp polarimeter, CH_2 ... target of the pp polarimeter, F4, F5 ... focal points

BT contained 20 cm Be, its cross section being 8×8 cm^2. Energy losses of deuterons during their passage through air, foils in vacuum tubes of the beam transport line and the BT matter, provided a decrease of the deuteron beam energy of 20 MeV in the BT center. The mean neutron energy thus decreases by 10 MeV [3,5]. For the $\Delta\sigma_{\rm L}$ results the energies in the BT center were taken into account, whereas for the beam polarization measurements the extracted beam energies have been used.

The values and directions of the neutron and proton polarizations after break-up, $\mathbf{P}_{\rm B}(n)$ and $\mathbf{P}_{\rm B}(p)$, respectively, are the same as the vector polarization $\mathbf{P}_{\rm B}(d)$ of the incident deuteron beam [36,37].

In our previous experiments [3–6] the deuteron beam polarization was determined by two independent asymmetry measurements, either for the dp elastic, or for the pp quasielastic reactions. In the first case, a four-arm beam line polarimeter [32] was used and deuterons, scattered on the liquid hydrogen target, were analyzed by a magnetic field. This polarimeter was used in the primary deuteron beam line. It accurately determined the elastic dp scattering asymmetry at $T_{\rm kin}(d) = 1.60$ GeV, where the analyzing power of this reaction is well known [38]. In principle, the $P_{\rm B}(d)$ needs to be determined at one energy only, since no deuteron depolarizing resonance at the Synchrophasotron exists [32]. On the other hand, the measurements require changing the deuteron energy and extracting deuterons in another beam line, which is a time-consuming operation. For this reason the dp polarimeter was not used in the 2001 run. In [5,6] we obtained an average for positive and negative signs of the vector polarization $|P_{\rm B}(d)| = 0.524 \pm 0.010({\rm stat}) \pm 0.010({\rm syst})$.

Another four-arm beam polarimeter [33] with small acceptance of 7.1×10^{-4} sr continuously monitored $P_{\rm B}(p)$ value during the data acquisition. The deuteron beam, considered as a beam of quasifree protons and neutrons, was scattered on CH_2 target at 14° lab. This polarimeter measured the pp left-right asymmetry on hydrogen and carbon at $T_{\rm kin}(p) = T_{\rm kin}(d)/2$ and the pC asymmetry was subtracted. The polarimeter was calibrated and improved [39,40]. The results obtained by this polarimeter yilded deuteron beam polarization $|P_{\rm B}(d)|$ values, averaged over different parts of the data taking. These values were taken into account in the data treatment. The weighted average over the entire 2001 run gives $|P_{\rm B}(d)| = 0.528 \pm 0.004({\rm stat}) \pm 0.008({\rm syst})$, and agree with our previous dp polarimeter results.

The dimensions and positions of the iron and brass collimators C1–C4 (Fig. 1) were as described in [3,4]. Accurate measurements of the collimated neutron beam profiles were performed in a special run, using nuclear emulsions. During the data acquisition, the positions and X-Y profiles were monitored by the neutron beam profile monitor NP. It was equipped with multiwire proportional chambers and placed close downstream from the last transmission detector.

In order to change the vertical orientation of the neutron beam polarization to the longitudinal direction, a spin-rotating magnet (SRM) was used. The SRM magnetic field map was accurately measured. The uncertainty of the magnetic field integral within the neutron beam path area may provide a small additional systematic error of ±0.2 %. The magnetic field value was continuously monitored by a Hall probe, since a high stability of SRM is needed.

The frozen-spin PPT, reconstructed to be a movable device [10–12] was used. The target material was 1-pentanol ($C_5H_{12}O$ + 5 % H_2O) with a paramagnetic Cr^V impurity (EHBA) having a spin concentration of 7×10^{19} cm^{-3}. Pentanol beads were loaded in a thin-wall teflon container 200 mm long and 30 mm in diameter, placed inside the dilution refrigerator. The weight of the pentanol beads was (80.1 ± 0.05) g and the total number of polarizable hydrogen atoms on the beam neutron path was $n_{\rm H} \times d = (9.14 \pm 0.10)\ 10^{23}$ cm^{-2}.

The PPT polarization $P_{\rm T}$ was measured using a computer-controlled NMR system. These measurements were carried out at the beginning and at the end of data taking for each sign of the PPT polarization. The negative and positive target proton polarizations were about –0.75 and 0.60, respectively. The relaxation times were more than 5000 hours for $P_{\rm T}^-$ and 7000 hours for $P_{\rm T}^+$. The relative uncertainty of the measured $P_{\rm T}$ values has been estimated at ±5 %. This uncertainty includes the errors of polarization uniformity measurements, using NMR data from three coils placed inside the PPT container along the target length. For the processing of accumulated data, the $P_{\rm T}$ time dependence was taken into account.

The configuration of the two neutron intensity monitors M1 and M2 and the three transmission detectors T1, T2 and T3 is shown in Fig. 2. Each of the detectors has to

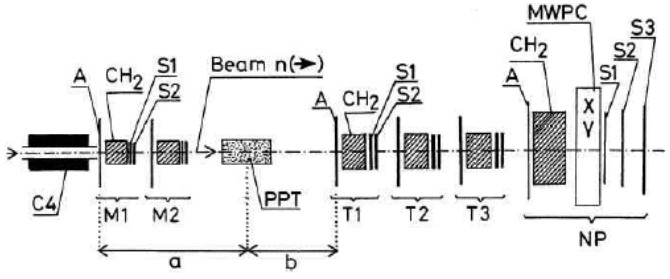

Fig. 2. Experimental set-up for the $\Delta\sigma_{\rm L}(np)$ measurement (not in the scale). The meaning of the symbols: C4 ... last neutron beam collimator, 25 mm in diameter, M1, M2 ... monitor neutron detectors, T1, T2, T3 ... transmission neutron detectors, NP ... neutron beam profile monitor, CH_2 ... converters (dimensions in text), A ... anticoincidence scintillation counters, S1, S2, S3 coincidence scintillation counters, MWPC ... two multi-wire proportional chambers, distance a = 235 cm, distance b = 655 cm

be independent of any other. All the units were of similar design [15] and the electronics were identical, as described in [3,4]. Each unit consisted of a CH_2 converter, 60 mm thick, placed behind the large veto scintillation counter A. The emitted forward charged particles, generated by neutron interactions in the converter matter, were detected by two counters S1 and S2 in coincidence. The converters and S1, S2 counters for monitors M1 and M2 were 30 mm in diameter and the corresponding elements for the transmission detectors T1, T2 and T3 were 90, 92 and 94 mm, respectively. Each of the neutron detector used provides a very good stability of detection efficiency. The efficiencies of $\approx$ 2 % for all detectors are practically constant with energy.

The NP array, also shown in Fig. 2, was similar to the neutron detectors. The two multiwire proportional chambers behind the converter were protected by veto A of the NP array and triggered by S1, S2 and S3 counters in coincidence.

The result of $\Delta\sigma_{\rm L}$ is independent of the neutron beam intensity, if the probability of quasi-simultaneous detection of two neutrons in one detector unit may be considered negligible. The small detection efficiencies decrease the probability for a converted neutron to be accompanied by another quasi-simultaneous converted neutron in the same detector. "Simultaneous" detection is to be understood as occuring within the resolution time of a scintillation counter. The probability was estimated from results obtained with different neutron beam intensities and different radiator thickness [15,16]. For the same neutron fluxes, the probability increases quadratically with increasing detector efficiency. At high efficiencies (namely for *pp* transmission experiments) it represents the dominant source of systematic errors. This effect of "simultaneous" detection of two neutrons in one detector unit, was estimated to be smaller than 2×10^{-6} in the present experiment.

A misalignment of the detector components or of the entire detectors provide instrumental asymmetry IA. To reach a perfect alignment is beyond experimental possibility. In the case of misalignment, the asymmetries in each neutron detector depend on the transverse beam polarization components only. For "T" detectors the misalignment effects are practically independent of the target polarizations [41,15]. The instrumental asymmetry IA in (2.7) may be of the same order or larger than the transmission effects and provides the same contribution to each pair of measurements in (2.5a) or (2.5b). It is obvious that this effect will be considerably stronger for the $\Delta\sigma_{\rm T}$ measurement than for the $\Delta\sigma_{\rm L}$ one, where only residual perpendicular $P_{\rm B}$ components exist. These undesirable components depend on the accuracy of the SRM current setting. As already mentioned, IA cancels out when taking the simple average of results in (2.8). The results strongly depend on the detector stabilities and their fixed positions over the data acquisition with both $P_{\rm T}$ signs.

However, there are small random-like instrumental effects (RLE), provided e.g. by temperature, magnetic field fluctuations, beam position variations, etc. They affect the stability of set-up elements in an uncontrolled manner. For the final $\Delta\sigma_{\rm L}$ results, uncertainties provided by RLE were estimated using a special procedure of data treatment (see Sect. 5).

A possible inefficiency of protection against charged particles by all veto counters may exist. Charged particles in the neutron beam are produced mainly in beam collimators, in CH_2 radiators of all M and T detectors, and in the target. Only a small fraction of the forward protons is polarized. They are produced in the polarized target by elastic scattering of polarized neutrons on free polarized protons in a vicinity of $\theta_{\rm CM}(n) = 180°$. For the longitudinally polarized beam and target one obtains a contribution from the spin correlation parameter $A_{ookk}(np)$ [26], which is included in the counting rate asymmetry for the observable $\Delta\sigma_{\rm L}$. This additional asymmetry was calculated in [3,4] and may provide a ± 0.1 % systematic error. Let us note that $A_{ookk}(180°,\ np)$ is one of the observables which determine the real parts of the forward scattering amplitudes for the isospin I = 0 state [31].

For the measured $\Delta\sigma_{\rm L}$ values, the relative normalization and systematic errors from different sources are summarized as follows:

– Beam polarization over the run	± 0.9 %
– Target polarization	± 5.0 %
– Number of the polarizable hydrogen atoms	± 1.1 %
– Polarization of other atoms	± 0.3 %
– Magnetic field integral of the neutron spin rotator	± 0.2 %
– Inefficiencies of veto counters	± 0.1 %
– Total of the relative systematic errors	± 5.3 %
– Absolute error due to the extrapolation of results towards 0°	< 0.04 mb

Tests of the experimental set-up were performed during additional runs with high intensity unpolarized deuteron beams, extracted either from the Synchrophasotron, or from the Nuclotron. The unpolarized neutron

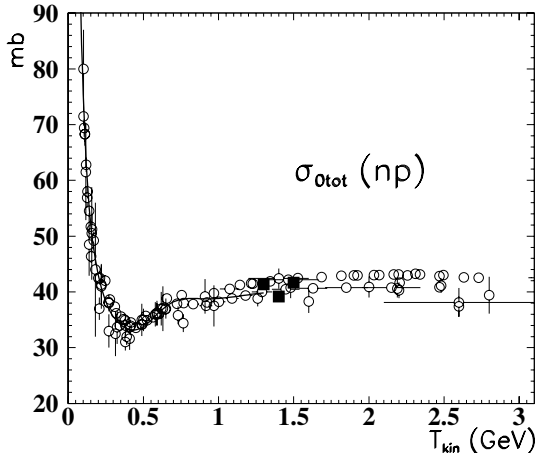

Fig. 3. Energy dependence of $\sigma_{0\rm tot}(np)$. The meaning of the symbols: open circles ... world data from [42–44], black squares ... this experiment, solid curve ... ED GW/VPI-PSA [47] (SP03 solution)

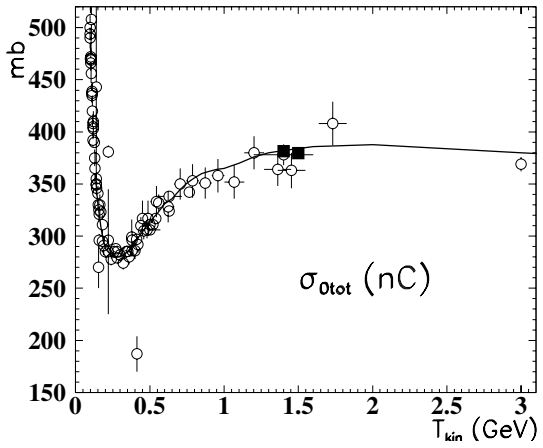

Fig. 4. Energy dependence of $\sigma_{0\rm tot}(n{\rm C})$. The meaning of the symbols: open circles ... world data from [45], black squares ... this experiment, solid curve ... [45]

Table 1. Unpolarized total cross sections for np and nC interactions

$T_{\rm kin}(n)$ (GeV)	$\sigma_{0\rm tot}(np)$ (mb)	$\sigma_{0\rm tot}(n{\rm C})$ (mb)
1.30 ± 0.013	41.35 ± 0.66	–
1.40 ± 0.014	39.18 ± 0.48	381.5 ± 2.6
1.50 ± 0.015	41.63 ± 0.83	379.6 ± 1.0

beam energies were 1.3, 1.4 and 1.5 GeV. We used the same transmission set-up as described above, where PPT was removed and either liquid hydrogen, or carbon targets were inserted in the neutron beam line. Transmission ratios were completed by corresponding empty target data. These measurements allowed to determine the total cross sections $\sigma_{0\rm tot}(np)$ and $\sigma_{0\rm tot}(n{\rm C})$. For nC experiment at $T_{\rm kin}(n) = 1.5$ GeV, the transmission was measured using several carbon targets with different thicknesses. The results obtained for the two total cross sections are summarized in Table 1.

Our results are shown in Figs. 3, 4, where they are compared with existing data, listed in compilations [42–44] for np and in [45] for nC interactions.

5 Data analysis

For each accelerator cycle the following main information was recorded and displayed by the data acquisition system:

- rates of the two calibrated ionization chambers used as primary deuteron beam intensity monitors,
- rates of coincidences and accidental coincidences for the two neutron detectors M1 and M2 used as intensity monitors of the neutron beam incident on the PPT,
- rates of coincidences and accidental coincidences for the three neutron transmission detectors T1, T2 and T3,
- rates of the left and right arms of the pp beam polarimeter.

At the beginning of the run, statistics at $T_{\rm kin} = 1.4$ GeV with $P_{\rm T}^{+}$ and $P_{\rm T}^{-}$ were recorded. Then the data were taken at 1.7, 2.0 and 1.9 GeV with $P_{\rm T}^{-}$. Finally, the data were acquired at 1.9, 2.0 and 1.7 GeV with $P_{\rm T}^{+}$.

The recorded data were then analyzed in three steps. In the first step, the data were cleaned of low-quality information. To start with, the "bad" data files were removed. Then the data files were cleaned of the "bad" cycles with an absence or incorrect sequence of labels of $P_{\rm B}$ signs. The number of such "bad" cycles for the cumulated statistics represents a few tenth of one percent. The data were also cleaned of the cycles with no beam at all ("empty" cycle), or a low level beam intensity and/or with an abnomal fluctuation of the neutron detector characteristics. The main part of all "bad" cycles ($\sim 5\%$) was rejected due to the low intensity of the neutron beam. Remaining event statistics over the run at a given energy and for each combination of the $\mathbf{P}_{\rm B}$ and $\mathbf{P}_{\rm T}$ directions were used to determine $\Delta\sigma_{\rm L}$ and IA. The transmission ratios from (3.3) averaged over the beam and target polarizations are proportional to $\sigma_{0\rm tot}({\rm PPT})$ for the target material. The transmission ratios were listed in [5,6] at three energies and are not shown here, since the conclusions are identical. In the energy region under discussion $\sigma_{0\rm tot}({\rm PPT})$ slightly decreases with decreasing energy. A monotonous decrease of $\sigma_{0\rm tot}({\rm PPT})$ as a function of the distance of the neutron transmission detector from the target was also observed, as expected.

The second and third steps of the data analysis used the previously selected events. The stabilities of the SRM magnetic field and of the neutron detectors were checked, the parameters of statistical distributions of the $\Delta\sigma_{\rm L}$ results were determined for all pairs of the following cycles with $P_{\rm B}^{+}$ and $P_{\rm B}^{-}$, and the final results were obtained. The transmission ratios as functions of time were analyzed for each combination of the individual M and T detectors, at any neutron energy and for both $P_{\rm T}$ signs. No signif-

icant time dependence of checked values and no sizeable deviations from normal distributions were observed.

The $\Delta\sigma_{\rm L}$ values over a given run were calculated by two different methods. In the first method, the $\Delta\sigma_{\rm L}$ values were obtained using (3.4a),(3.4b) and (3.5) for entire event statistics of each neutron detector (M1,M2,T1,T2,T3), acumulated over the run. In the second method, first the partial $\Delta\sigma_{\rm L}$ values and their statistical errors were calculated from the individual neutron detector statistics for each "pair" of the following cycles with the opposite beam polarizations $P_{\rm B}^{+}$ and $P_{\rm B}^{-}$. The relations (3.4a,b), (3.5) were used again and the time dependent sequence of recorded cycles is known. Thus obtained partial $\Delta\sigma_{\rm L}$ values and their statistical errors for all "pairs" were added using the weighted mean procedure. The second method takes into account both the statistical uncertainties and the "random-like" instrumental effects RLE.

The final results of the data treatment are presented in Table 2. The $-\Delta\sigma_{\rm L}$ values at four energies measured with the individual transmission detectors T1,T2,T3 for both signs of $P_{\rm T}$, their half-sums from (2.8) and half-differences, i.e. the hidden contributions IA [15] from (2.7), are listed. The results were obtained using combined statistics from the two monitors M1 and M2. The T123 value at any energy represents the weighted average of the three transmission detector contributions.

The $-\Delta\sigma_{\rm L}$ and their experimental errors given in Table 2 have been calculated by the second ("pair") method, In order to estimate the RLE contribution to the experimental error we calculated the ratio

$$\mathrm{R} = \delta_{\text{"pair"}}/\delta_{\rm stat} \geq 1 \ , \qquad (5.1)$$

where $\delta_{\text{"pair"}}$ is the error obtained by the second method and $\delta_{\rm stat}$ is the error obtained by the first one. The value of R = 1 occurs if no RLE exists and it increases with increasing RLE. In our experiment the errors of the final results obtained by the "pair" method exceed the statistical errors obtained from (3.5) by ≈ 4 % (see last column in Table 2).

As can be seen from Table 2, the IA values at 1.39 and 1.69 GeV are positive, whereas at 1.89 and 1.99 GeV they are mostly negative. Since the neutron detectors were not moved during the run, we assume that the residual perpendicular components in $\mathbf{P}_{\rm B}$ were opposite.

6 Results and discussion

The final $-\Delta\sigma_{\rm L}(np)$ values are presented in Table 3 and shown in Fig. 5. Experimental ($\delta_{\text{"pair"}}$) and systematic errors are taken into account. Total errors are quadratic sums of both uncertainties.

Table 2. Measured $-\Delta\sigma_{\rm L}(np)$ values at different neutron beam energies $T_{\rm kin}(n) = T_n$ GeV for two opposite target polarizations, for individual transmission detectors (T1,T2,T3) and for entire recorded statistics (T123). The data were calculated using the procedure of average weighting of the results for each pair of the following cycles with opposite beam polarizations $P_{\rm B}^{+}$ and $P_{\rm B}^{-}$. Therefore the errors quoted take into account both the statistical uncertainties and the "random-like" instrumental effects. Since the IA and the average $-\Delta\sigma_{\rm L}(np)$ values have the same experimental errors they are indicated for the $-\Delta\sigma_{\rm L}(np)$ values only. The R-values (see text) check the importance of RLE

T_n	TD	$-\Delta\sigma_{\rm L}(P_{\rm T}^{+})$ (mb)	$-\Delta\sigma_{\rm L}(P_{\rm T}^{-})$ (mb)	IA (mb)	Average $-\Delta\sigma_{\rm L}$ (mb)	R
1.39	T1	$+12.14 \pm 3.09$	$+3.33 \pm 2.48$	$+4.41$	$+7.73 \pm 1.98$	1.195
	T2	$+10.83 \pm 3.17$	$+2.92 \pm 2.56$	$+3.95$	$+6.87 \pm 2.04$	1.204
	T3	$+7.73 \pm 3.28$	$+1.23 \pm 2.65$	$+3.25$	$+4.48 \pm 2.11$	1.211
	T123	$+10.32 \pm 1.83$	$+2.54 \pm 1.48$	$+3.69$	$+6.43 \pm 1.18$	1.036
1.69	T1	$+2.53 \pm 2.04$	$+0.68 \pm 1.58$	$+0.92$	$+1.60 \pm 1.29$	1.190
	T2	$+4.51 \pm 2.09$	-1.65 ± 1.62	$+3.08$	$+1.43 \pm 1.32$	1.197
	T3	$+6.08 \pm 2.17$	$+0.86 \pm 1.68$	$+2.61$	$+3.47 \pm 1.37$	1.203
	T123	$+4.30 \pm 1.21$	-0.41 ± 0.94	$+2.17$	$+2.13 \pm 0.77$	1.037
1.89	T1	$+3.47 \pm 2.34$	$+3.08 \pm 2.46$	$+0.20$	$+3.27 \pm 1.70$	1.272
	T2	-0.84 ± 2.41	$+2.40 \pm 2.54$	-1.62	$+0.78 \pm 1.75$	1.284
	T3	$+1.17 \pm 2.49$	$+4.74 \pm 2.63$	-1.78	$+2.96 \pm 1.81$	1.295
	T123	$+1.31 \pm 1.39$	$+3.37 \pm 1.47$	-1.03	$+2.34 \pm 1.01$	1.043
1.99	T1	$+0.76 \pm 2.03$	$+2.87 \pm 1.85$	-1.06	$+1.82 \pm 1.37$	1.222
	T2	-1.47 ± 2.09	$+3.82 \pm 1.90$	-2.64	$+1.17 \pm 1.41$	1.230
	T3	$+0.71 \pm 2.16$	$+2.35 \pm 1.97$	-0.82	$+1.53 \pm 1.46$	1.239
	T123	$+0.00 \pm 1.21$	$+3.03 \pm 1.10$	-1.51	$+1.51 \pm 0.82$	1.030

Table 3. Final $-\Delta\sigma_{\rm L}(np)$ results. Total errors are quadratic sums of the experimental ("pair") and systematic errors. Laboratory kinetic energies and momenta of the neutron beam in the production target center are given

$T_{\rm kin}(n)$ (GeV)	$p_{\ell ab}(n)$ (GeV/c)	$-\Delta\sigma_{\rm L}(np)$ (mb)	Experim. error (mb)	System. error (mb)	Total error (mb)
1.39	2.13	+6.43	±1.18	±0.34	±1.23
1.69	2.46	+2.13	±0.77	±0.11	±0.78
1.89	2.67	+2.34	±1.01	±0.12	±1.02
1.99	2.77	+1.51	±0.82	±0.08	±0.82

The results from [3–6] together with the existing $-\Delta\sigma_{\rm L}(np)$ data [15,16,18,19], obtained with free polarized neutrons below 1.1 GeV, are also plotted in Fig. 5. In [5] we added the TUNL point at 19.7 MeV [24] and the PSI point at 66 MeV [20], in order to show the $-\Delta\sigma_{\rm L}(np)$ energy dependence and existing structure at low energies. This structure (not shown here) was described in the energy dependent (ED) GW/VPI phase shift analysis (PSA) (solution SP99, [46]) and is described again using the recent solution SP03 of the same PSA [47]. In the present paper we discuss mainly the energy dependence over the high energy region.

The new *np* results agree with our previous data, confirming a fast decrease above 1.1 GeV, and suggesting a minimum or a shoulder in the vicinity of 1.8 GeV. The solid curve represents the fit of $-\Delta\sigma_{\rm L}(np)$ from the SP03 solution [47] below 1.3 GeV. Above 0.6 GeV the PSA fit is only in qualitative agreement with the measured values.

From (2.12) we deduced $-\Delta\sigma_{\rm L}({\rm I}=0)$, using the obtained $-\Delta\sigma_{\rm L}(np)$ results and the corresponding *pp* values at the same energies. In order to determine $-\Delta\sigma_{\rm L}(pp)$ we used different sources:

- Calculations using ED GW/VPI PSA [47] (solution SP03).
- Linear interpolation of the fixed energy (FE) GW/VPI PSA [47] results, using the solutions at 1.275, 1.50, 1.70, 1.80, 1.95, and 2.025 GeV.
- Linear interpolation of the FE Saclay-Geneva (SG) PSA results [30], using the solutions at 1.3, 1.6, 1.8 and 2.1 GeV.
- Interpolation of the *pp* experimental data measured at ANL-ZGS [48,49] and Saturne II [50] in the vicinity of *np* energies.

The four calculated *pp* data sets are listed in the upper part of Table 4. Let us note that from ED GW/VPI PSA no errors could be calculated and in FE GW/VPI PSA they are obviously overestimated. In FE SG PSA the errors are calculated using the error matrix, and are compatible with those obtained by the direct interpolation of neighboring measured values.

The results of $-\Delta\sigma_{\rm L}({\rm I}=0)$, using the four sets of *pp* values are given in the bottom part of Table 4. We have added the SG PSA errors to the ED GW/VPI *pp* predictions. The results at each energy agree within the errors. Since, in general, the *pp* data are accurate, the $-\Delta\sigma_{\rm L}({\rm I}=0)$ values have roughly two times larger errors than the *np* results. For this reason, an improved accuracy of *np* measurements is important.

The new $-\Delta\sigma_{\rm L}({\rm I}=0)$ results, calculated with ED GW/VPI *pp* values are plotted in Fig. 6, together with

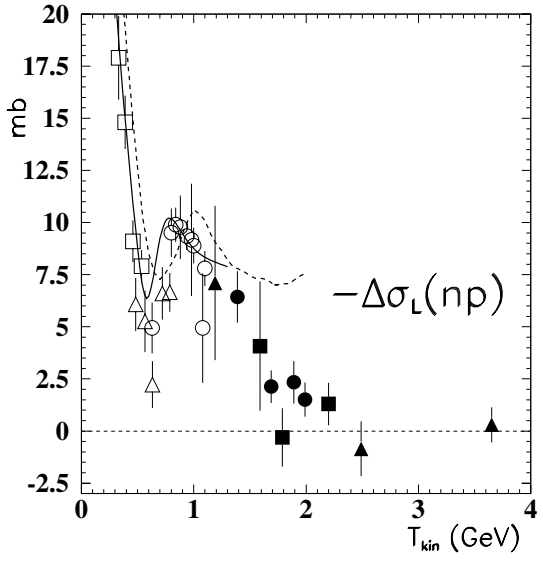

Fig. 5. Energy dependence of $-\Delta\sigma_{\rm L}(np)$. The meaning of the symbols: black dots ... this experiment, black triangles ... JINR [3,4], black squares ... JINR [5,6], open squares ... PSI [18], open triangles ... LAMPF [19], open circles ... Saturne II [15,16], solid curve ... ED GW/VPI PSA [47] (SP03 solution), dashed curve ... meson-exchange model [51]

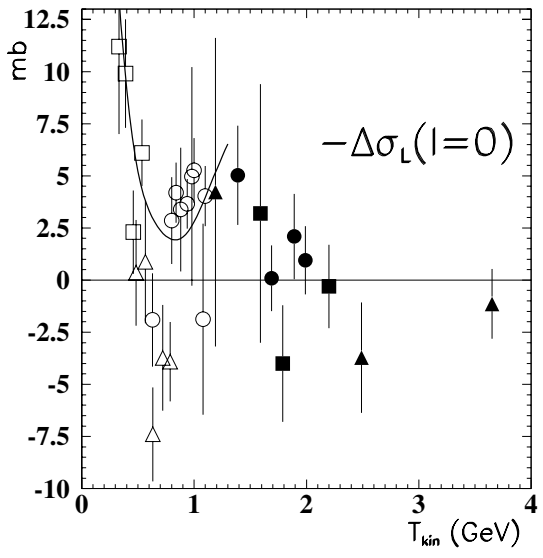

Fig. 6. Energy dependence of the $-\Delta\sigma_{\rm L}({\rm I}=0)$ calculated from the measured *np* data and the corresponding *pp* values from [47], solution SP03. The *np* data at the same energies as in Fig. 5 are used and the I = 0 results are labeled by the same symbols. The solid curve is calculated from the common *np* and *pp* ED GW/VPI PSA [47] (SP03 solution)

Table 4. Upper part: $-\Delta\sigma_{\rm L}(pp)$ values deduced from the four sources. Lower part: Four sets of $-\Delta\sigma_{\rm L}({\rm I}=0)$ results, calculated from the present *np* data and corresponding *pp* values

$T_{\rm kin}$ (GeV)	$-\Delta\sigma_{\rm L}(pp)$ (mb) ED GW/VPI	$-\Delta\sigma_{\rm L}(pp)$ (mb) FE GW/VPI	$-\Delta\sigma_{\rm L}(pp)$ (mb) FE SG	$-\Delta\sigma_{\rm L}(pp)$ (mb) data interpol.
1.39	$+7.83$	$+7.73 \pm 2.13$	$+7.82 \pm 0.30$	$+6.45 \pm 0.53$
1.69	$+4.17$	$+4.14 \pm 1.71$	$+4.35 \pm 0.30$	$+3.78 \pm 0.30$
1.89	$+2.60$	$+1.87 \pm 2.27$	$+3.09 \pm 0.30$	$+2.77 \pm 0.18$
1.99	$+2.07$	$+0.44 \pm 2.21$	$+2.82 \pm 0.20$	$+2.20 \pm 0.18$
$T_{\rm kin}$ (GeV)	$-\Delta\sigma_{\rm L}({\rm I}=0)$ (mb)	$-\Delta\sigma_{\rm L}({\rm I}=0)$ (mb)	$-\Delta\sigma_{\rm L}({\rm I}=0)$ (mb)	$-\Delta\sigma_{\rm L}({\rm I}=0)$ (mb)
1.39	$+5.03 \pm 2.38$	$+5.13 \pm 3.18$	$+5.04 \pm 2.38$	$+6.43 \pm 2.41$
1.69	$+0.09 \pm 1.58$	$+0.12 \pm 2.29$	-0.09 ± 1.58	$+0.18 \pm 1.58$
1.89	$+2.09 \pm 2.05$	$+2.82 \pm 3.04$	$+1.60 \pm 2.05$	$+1.92 \pm 2.03$
1.99	$+0.95 \pm 1.64$	$+2.59 \pm 2.75$	$+0.21 \pm 1.64$	$+0.82 \pm 1.64$

other existing data in a large energy interval. The solid curve was calculated from *np* and *pp* ED GW/VPI PSA predictions below 1.3 GeV ([47] solution SP03). Above 0.5 GeV the PSA solution is not in agreement with the data. The energy dependences of the isovector part $-\Delta\sigma_{\rm L}(pp)$, calculated from ED GW/VPI (([46] solution SP99) and from SG PSA [30] have been shown in [5,6] and will not be repeated here.

The new $-\Delta\sigma_{\rm L}({\rm I}=0)$ results agree again with our previous data, confirming a plateau around 1.4 GeV, followed by a fast decrease and suggesting a minimum in the vicinity of 1.8 GeV. This structure is better pronounced than the similar one in the $-\Delta\sigma_{\rm L}(np)$ energy dependence.

Some dynamic models predicted the $-\Delta\sigma_{\rm L,T}$ energy behaviour for *np* and *pp* interactions. Below 2.0 GeV, an usual meson exchange theory of NN scattering [51] gives the $-\Delta\sigma_{\rm L}(np)$ energy dependence as shown by the dashed curve in Fig. 5. It can be seen that this model provides only a qualitative description at low energies and disagrees considerably with the data above 1 GeV.

In [3,4,6] we discussed the model of a nonperturbative flavour-dependent interaction between quarks, induced by a strong fluctuation of vacuum gluon fields, i.e. instantons. Concerning this model, we refer to our previous papers, since no new relevant predictions are available. The former prediction at high energy [6] disagree with the experimental data.

The investigated energy region corresponds to a possible generation of heavy dibaryons with masses M > 2.4 GeV (see review [52]). For example, the model [53, 54] predicts the formation of a heavy dibaryon state with a color octet-octet structure.

The possible manifestation of exotic dibaryons in the energy dependence of different *pp* and *np* observables was predicted by another model [55–59]. The authors used the Cloudy Bag Model and an R-matrix connection to long-range meson-exchange force region with the short-range region of asymptotically free quarks. In [59] the prediction of $-\Delta\sigma_{\rm L}(np)$ as a function of the neutron beam energy is shown. The prediction is valid below 0.9 GeV only, and is irrelevant for our purposes. On the other hand, this hybrid model gives the lowest lying exotic six-quark configurations in the isosinglet $^3{\rm S}_1$ state with the mass M = 2.63 GeV ($T_{\rm kin}(n) = 1.81$ GeV). It is close to the energy where the structure is suggested by our results.

The observed minimum in the excitation function of $-\Delta\sigma_{\rm L}(np)$ near 1.8 GeV (see Fig. 5) is only a two standard deviation effect. We stress that it can be the result of a statistical fluctuation, which occurs more frequently in the inclusive experiments than in exclusive ones. The same statement holds for the $-\Delta\sigma_{\rm L}({\rm I}=0)$ energy dependence (Fig. 6), which is dependent on the $-\Delta\sigma_{\rm L}(np)$ measurements.

For a study of resonances the PSA procedure is one of the existing effective tools. To determine real and imaginary parts of the I = 0 phase shifts, a complete set of *np* and *pp* elastic scattering observables needs to be measured over the entire angular region at a given energy. The existing data allow to perform *np* PSA below 1.1 GeV only, whereas the *pp* data for the same purpose are sufficient up to 2.7 GeV. Measurements of the complete *np* data sets at any energy above 1.1 GeV is an impossible task within our experimental conditions. Only few observables could be determined in the forward and backward directions.

The partial DRSA analysis for the imaginary parts of the forward amplitudes was treated in Sect. 2. The corresponding real parts can be determined by measurements of selected *np* elastic scattering observables in the experimentally accessible backward direction, as was shown in [31]. A complete DRSA for (I = 0) would allow to discuss possible energy-dependent structures on the the level of complex scattering amplitudes and and not only on the level of observables.

Below we summarize, what may be deduced from the existing and planned $\Delta\sigma_{\rm L,T}(np)$ experiments.

Since $-\Delta\sigma_{\rm T}$ for arbitrary isospin state contains no uncoupled spin-triplet contribution, a possible $^3{\rm S}_1$ resonance effect in this observable may be less diluted by other spin-

states than in $-\Delta\sigma_{\rm L}$. The measurement of $-\Delta\sigma_{\rm T}(np)$ and the determination of the $-\Delta\sigma_{\rm T}({\rm I}=0)$ energy dependence may provide a significant and sensitive check of the predicted resonance. Moreover, in any difference $\Delta\sigma_{\rm L}-\Delta\sigma_{\rm T}$ the spin-singlet contributions vanish. For this reason, the accurate $-\Delta\sigma_{\rm L,T}(np)$ measurements, in small energy steps, near to $T_{\rm kin}(n)=1.8$ GeV are desirable.

The I = 0 spin dependent total cross section differences represent a considerable advantage for studies of the $^3{\rm S}_1$ state around 1.8 GeV, since this partial wave is expected to be dominant. This is in contrast with the I = 1 system, where the lowest lying exotic six-quark configuration was predicted in the spin-singlet state $^1{\rm S}_0$ above 2 GeV [59]. This state is not dominant and is strongly diluted in the forward direction. On the other hand, it has to be emhasized that a search for a narrow I = 0 resonance needs much higher accuracies of the observable $-\Delta\sigma_{\rm L}({\rm I}=0)$ than presently available.

7 Conclusions

New results, obtained in the transmission experiment, complete the measurement of the $-\Delta\sigma_{\rm L}(np)$ energy dependence at the Dubna Synchrophasotron. Measured $-\Delta\sigma_{\rm L}(np)$ values are compatible with the existing np results, using free neutrons. The rapid decrease of $-\Delta\sigma_{\rm L}(np)$ values above 1.1 GeV is confirmed and a minimum or a shoulder around 1.8 GeV is observed.

The $-\Delta\sigma_{\rm L}({\rm I}=0)$ quantities, deduced from the measured $-\Delta\sigma_{\rm L}(np)$ values and the existing $-\Delta\sigma_{\rm L}(pp)$ data, are also presented. They indicate a plateau or a weak maximum around 1.4 GeV, followed by a rapid decrease with energy and by a minimum around 1.8 GeV.

The obtained results are compared with the dynamic model predictions and with the recent ED GW/VPI PSA fit. The necessity of further accurate $-\Delta\sigma_{\rm L}(np)$ measurements around 1.8 GeV and new $-\Delta\sigma_{\rm T}(np)$ data in the kinetic energy region above 1.1 GeV is emphasized.

The spin-dependent results were completed by the measurements of unpolarized total cross sections $\sigma_{0{\rm tot}}(np)$ and $\sigma_{0{\rm tot}}(n{\rm C})$. The data were obtained using the unpolarized deuteron beams extracted from the Synchrophasotron and the Nuclotron at several energies.

Acknowledgements. The autors are grateful to the Synchrophasotron–Nuclotron accelerator complex staff and all the scientific or engineering groups and individuals who took part and helped us during the $\Delta\sigma_{\rm L}$ measurements preparation, data taking, and data analyses. The authors also thank the JINR, VBLHE and DLNP directorates for the support granted to the investigations. During the last two years, this work was partly financed by the Russian Foundation for Basic Research, through Grant No 02-02-17129.

References

1. J. Ball et al.: in Proceedings of the International Workshop "Dubna Deuteron-91", JINR E2-92-25, p. 12, Dubna (1992)
2. E. Chernykh et al.: in Proceedings of the International Workshop "Dubna Deuteron-93", JINR E2-94-95, p. 185, Dubna (1994); Proceedings of the "V Workshop on High Energy Spin Physics", Protvino, 20–24 September 1993, p. 478, Protvino (1994)
3. B.P. Adiasevich et al.: Z. Phys. C **71**, 65 (1996)
4. V.I. Sharov et al.: JINR Rapid Communications **3[77]-96**, 13 (1996)
5. V.I. Sharov et al.: Eur. Phys. J. C **13**, 255 (2000)
6. V.I. Sharov et al.: JINR Rapid Communications **4[96]-99**, 17 (1999)
7. I.B. Issinsky et al.: Acta Physica Polonica B **25**, 673 (1994)
8. A. Kirillov et al.: *Relativistic Polarized Neutrons at the Laboratory of High Energy Physics, JINR*. Preprint JINR E13-96-210, Dubna (1996)
9. F. Lehar et al.: Nucl. Instrum. Methods A **356**, 58 (1995)
10. N.A. Bazhanov et al.: Nucl. Instrum. Methods A **372**, 349 (1996)
11. N.A. Bazhanov et al.: Nucl. Instrum. Methods A **402**, 484 (1998)
12. N.G. Anischenko et al.: JINR Rapid Communications **6[92]-98**, 49 (1998)
13. C. Lechanoine-Leluc, F. Lehar: Rev. Mod. Phys **65**, 47 (1993)
14. I.P. Auer et al.: Phys. Rev. Lett. **46**, 1177 (1981)
15. F. Lehar et al.: Phys. Lett. **189B**, 241 (1987)
16. J.-M. Fontaine et al.: Nucl. Phys. B **358**, 297 (1991)
17. J. Ball et al.: Z. Phys. C **61**, 53 (1994)
18. R. Binz et al.: Nucl. Phys. A **533**, 601 (1991)
19. M. Beddo et al.: Phys. Lett. **258B**, 24 (1991)
20. P. Haffter et al.: Nucl. Phys. A **548**, 29 (1992)
21. J. Brož et al.: Z. Phys. A **359**, 23 (1997)
22. W.S. Wilburn et al.: Phys. Rev. C **52**, 2352 (1995)
23. J. Brož et al.: Z. Phys. A **354**, 401 (1996)
24. J.R. Walston: Ph.D. Thesis, North Carolina State University (1998)
25. B.W. Raichle: Ph.D. Thesis, North Carolina State University (1997)
26. J. Bystrický, F. Lehar, P.Winternitz: J. Phys. (Paris) **39**, 1 (1978)
27. S.M. Bilenky, R.M. Ryndin: Phys. Lett. **6**, 217 (1963)
28. R.J.N. Phillips: Nucl. Phys. **43**, 413 (1963)
29. J. Ball et al.: Nuovo Cimento **111**, 13 (1998)
30. J. Bystrický, C. Lechanoine-Leluc, F. Lehar: Eur. Phys. J. C **4**, 607 (1998)
31. J. Ball et al.: Eur. Phys. J. C **5**, 57 (1998)
32. V.G. Ableev et al.: Nucl. Instrum. Methods A **306**, 51 (1991)
33. L.S. Azhgirey et al., Pribory i Tekhnika Experimenta **1**, 51 (1997) and transl. Instrum. Exp. Techiques **40**, 43 (1997)
34. N.V. Gorbunov, A.G. Karev: in Proceedings of the XII International Symposium on Nuclear Electronics, Varna, Bulgaria, September 12–18, 1988, JINR D13-88-938, p. 103, Dubna (1989)
35. V.G. Ableev et al.: Nucl. Phys. A **393**, 941 (1983) and Nucl. Phys. A **411**, 514E (1983)
36. E. Cheung et al.: Phys. Lett. B **284**, 210 (1992)
37. A.A. Nomofilov et al.: Phys. Lett. B **325**, 327 (1994)
38. V. Ghazikhanian et al.: Phys. Rev. C **43**, 1532 (1991)
39. L.S. Azhgirey et al.: Particles and Nuclei. Letts. **4[113]**, 51 (2002)

40. L.S. Azhgirey et al.: Nucl. Instrum. Methods A**497**, 340 (2003)
41. F. Perrot et al.: Nucl. Phys. B **278**, 881 (1986)
42. V.S. Barashenkov: *Cross Sections of Interactions of Elementary Particles*, Science, Moscow (1966)
43. J. Bystrický et al.: *Elastic and Charge Exchange Scattering of Elementary Particles a: Nucleon Nucleon and Kaon Nucleon Scattering*, Landolt-Börnstein, New Series, Vol. 9, editor H. Schopper, editor in Chief: K.H. Hellwege, Group I: Nuclear and Particle Physics, Springer-Verlag Berlin, Heidelberg, New York (1980)
44. J. Bystrický, F. Lehar: *Nucleon-Nucleon Scattering Data*, editors H. Behrens und G. Ebel, 1981 Edition, Fachinformationszentrum Karlsruhe, Nr.11-2 and Nr.11-3 (1981)
45. V.S. Barashenkov: *Cross Sections of Interactions of Particles and Nuclei with Nuclei*, JINR Publishing Dept., Dubna (1993)
46. R.A. Arndt et al.: Phys. Rev. C **56**, 3005 (1997)
47. R.A. Arndt, I.I. Strakovsky, R.L. Workman: Phys. Rev. C **62**, 034005 (2000)
48. I.P. Auer et al.: Phys. Rev. Lett. **41**, 354 (1978)
49. I.P. Auer et al.: Phys. Rev. D **34**, 2581 (1986)
50. J. Bystrický et al.: Phys. Lett. **142B**, 141 (1984)
51. T.-S.H. Lee: Phys. Rev. C **29**, 195 (1984)
52. I.I.Strakovsky: Fiz. Elem. Chastits At. Yadra **22**, 615 (1991), transl. Sov. J. Part. Nucl. **22**, 296 (1991)
53. B.Z. Kopeliovich, F. Niedermayer: Zh. Eksp. Teor. Fiz. **87**, 1121 (1984), transl. Sov. Phys. JETP **60**(4), 640 (1984)
54. B.Z. Kopeliovich: Fiz. Elem. Chastits At. Yadra **21**, 117 (1990), transl. Sov. J. Part. Nucl. **21**(1), 49 (1990)
55. P. LaFrance, E.L. Lomon: Phys. Rev. D **34**, 1341 (1986)
56. P. Gonzales, P. LaFrance, E.L. Lomon: Phys. Rev. D **35**, 2142 (1987)
57. P. LaFrance: Can. J. Phys. **68**, 1194 (1990)
58. E.L. Lomon: Colloque de Physique (France) **51**, C6-363 (1990)
59. P. LaFrance, E.L. Lomon: in Proceedings of the International Conference "Mesons and Nuclei at Intermediate Energies", Dubna, May 3–7, 1994, edited M.Kh. Khankhasaev and Zh.B. Kurmanov, p. 97 World Scientific, Singapore, (1995-XV)